THE ROLE OF INTERNAL STRESSES IN MICROWIRES ON THEIR SOFT MAGNETIC AND MICROWAVE ABSORBING CHARACTERISTICS[1]

X.F. Zheng[1], F.X. Qin[1,2], H. Wang[1], Y.-W. Mai[2] and H.X. Peng[1]

[1] Institute for Composites Science Innovation (InCSI), School of Materials Science and Engineering, Zhejiang University, Zheda Road, Hangzhou, 310027, PR. China
Email: zhengxuefei@zju.edu.cn, faxiangqin@zju.edu.cn

[2] Centre for Advanced Materials Technology (CAMT), School of Aerospace, Mechanical and Mechatronic Engineering, The University of Sydney, Sydney, NSW 2006, Australia

Keywords: Amorphous microwires, Microwire composites, Microwave absorption, Internal stress, Joule annealing

MS ID: 2310

ABSTRACT

A set of composite absorbers with ultra-low loading of down to 0.017 wt.% short- cut microwires were prepared and investigated in terms of their magnetic and microwave properties in the X-band (8-12 GHz). The key parameters that could factor into the performance of the present absorbers have been systematically studied from micro to macro scale, i.e., the domain structure modulated by different internal stress scenarios and relative importance of impedance matching and materials loss. 9 mm long wires after suitable treatment lead to the enhancement of microwave absorbing property mainly due to the larger magnetic loss resulted from the natural ferromagnetic resonance, which is induced in the domain rotation and reversal process. The internal stress modification by removal of glass and joule annealing has profound effects in formulating the microwave absorption frequency and intensity of microwires composites by tailoring the domain structure and local anisotropy field. It is found that the composites with microwires annealed at 132 mA for 15 min obtain the minimum reflection loss and broadest absorption bandwidth with reference to -10 dB at 1.5 mm thickness, which is -25.7 dB (0.81 GHz) at 11.39 GHz caused by the relative high attenuation constant and best matching condition where Z_{real} is 1.026 and Z_{imag} is -0.102. This indicates that impedance matching plays a dominant role in tailoring the microwave absorbing property. Remarkably, the unconventional absorption frequency - matching thickness relation violating the quarter-wavelength model offers possibility to address the limitation of thickness for low frequency absorbing application.

1 INTRODUCTION

With the rapid development of wireless communications, the working frequency of numerous consumer electronics has been shifted to the gigahertz range. To reduce the electromagnetic (EM) interference among different electronic devices, electromagnetic shielding or absorbing materials with a higher and wider working frequency range of significant microwave absorption, lower density, superior strength and smaller thickness are in high demand [1]. In recent years, composites with glass-coated ferromagnetic microwire inclusions have received much attention due to their high magnetic permeability from MHz to GHz frequency, which are promising for applications like sensor devices and electromagnetic absorbers [3-5]. Glass-coated microwires prepared by the technique of Taylor–Ulitovskiy have superior electromagnetic and mechanical properties and are the favorite fillers to form good interfaces with the resin since the surface tension of glass is much higher than that of the resin. It has been well established the internal stress plays a critical role in defining the magnetic structure and properties of amorphous microwires [3, 4]. The internal stresses come from two different sources, i.e.,

[1] **The short conference paper is excerpted and adapted from a full length manuscript under consideration for publication and it is not supposed to be publicized online.**

the glass cover and the rapid solidification process; they also vary at axial, radial and circumferential directions [5, 6]. Both glass removal and joule annealing [7] can effectively relieve the internal stress. In particular, appropriate joule annealing [8] can define better the microstructure and domain structure of the wires, which leads to optimized magnetic properties.

It is known that high permeability could reduce the electromagnetic penetration into the fibers at high frequency owing to the skin effect. Hence, such microwires with very fine thickness are desirable for shielding or absorbing purposes at high frequency. In another perspective, the aspect ratio and filling ratio of microwires play a significant role in governing the composite microwave absorption properties [9, 10]. According to our previous work, it's found that wires with larger aspect ratio (9 mm in length in present case) show the best microwave absorbing properties due to decreasing the depolarization factor and axial demagnetization factor, which result in dielectric resonance and natural ferromagnetic resonance (NFRM), respectively. However, it is noted that most reported composites filled with glass-coated microwires have excellent microwave absorption properties under the premise of a high filling ratio [5, 11]. How exactly soft magnetic properties of the microwires affect microwave absorption of composites filled with low loading of microwires remains to be revealed. Herein, we have prepared two sets of composites filled with as-cast microwires and with treated microwires by joule annealing and glass removal, respectively, to explore the detailed relationships between the microwave properties of the composites and magnetic properties of the microwires.

2 EXPERIMENTAL

2.1 Materials

Experimentally, the $Co_{60}Fe_{15}Si_{10}B_{15}$ glass-coated microwires with metallic nucleus diameter of 21 μm and glass coating thickness of 4 μm were made by a modified Taylor – Ulitovskiy technique[12] (see wire sample details in Table 1). 15 cm long glass-coated wires were annealed at 66 mA (AMW-66) and 132 mA (AMW-132) for 15 min, respectively. Electrical contacts were facilitated by mechanically removing the glass coating at the ends of the microwires. For glass removal (GRMW), 15 cm long microwires were etched in a HF acid solution and then washed by deionized water. All the microwires were cut into 9 mm length. For the microwires composites (see composites sample details in Table 2), the short wires were dispersed randomly in silicone rubber and then molded as cuboid samples with length of 22.86 mm, width 10.16 mm and thickness 5 mm, as shown in Fig. 1c. The composites were cured at 125 ^{o}C for 20 min.

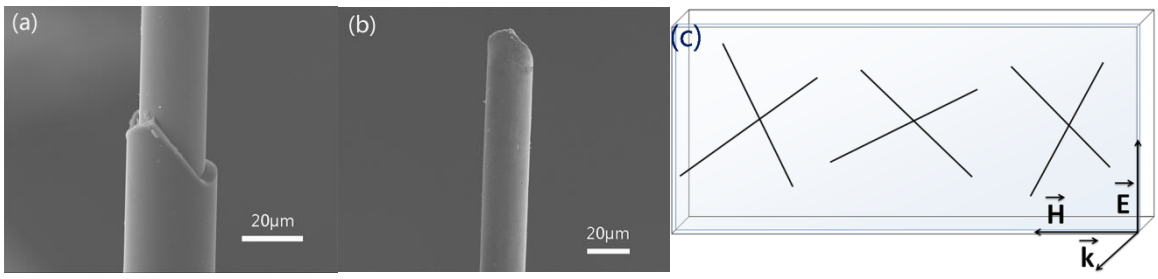

Fig. 1(Color online) (a) SEM images of glass - coated microwires, and (b) microwires after glass removal, (c) Composites embedded with 9 mm long microwires, n = 6, 0.017 wt.%

Sample	Metallic core (μm)	Glass coating (μm)	Annealing current (mA)	Annealing time (min)
MW	21	4	-	
GRMW	21	-	-	
AMW-66	21	4	66	15
AMW-132	21	4	132	15

Table 1 Parameters of microwires

Sample	microwires	Filling ratio (wt. %)	Wire length (mm)	Wire number	Topological arrangements
MC	MW	0.017	9	6	Shown in Fig.1c
GRMC	GRMW	0.017	9	6	Shown in Fig.1c
AMC-66	AMW-66	0.017	9	6	Shown in Fig.1c
AMC-132	AMW-132	0.017	9	6	Shown in Fig.1c

Table 2 Parameters of microwire composites

2.2 Characterization techniques

The morphology of microwires was investigated by scanning electron microscopy (SEM), Hitachi 3400, Japan. All the samples were analyzed by using a Shimadzu X-ray diffractometer 6000 with Cu-Ka radiation as a source. The magnetic hysteresis loops of the microwires were measured with a Quantum Design PPMS-VSM. Electromagnetic parameters (complex permeability μ and complex permittivity ε) of the composites were measured by the Rohde & Schwarz ZNB 40 vector network analyzer (VNA) using a waveguide in TE10 dominant mode frequency range WR-90 from 8 GHz to 12 GHz. The VNA was calibrated by the TRL (thru-reflect-line) method[13]. Microwave traveled via the silicone rubber layer first before penetrating the wire-composite layer. Permittivity and permeability were calculated by the Nicholson Ross Weir (NRW) method [14] from the measured scattering parameters from VNA. The microwave properties of the materials were evaluated by the reflection loss, which can be calculated based on the complex permeability and complex permittivity according to the transmission line theory [15]. The reflection loss, *RL*, can be calculated by [16]

$$Z = Z_{in}/Z_0 = (\mu_r/\varepsilon_r)^{1/2} \tanh[j(2\pi fd/c)(\mu_r\varepsilon_r)^{1/2}]; \quad (1)$$

$$RL = 20\log\left|(Z\text{-}1)/(Z+1)\right|, \quad (2)$$

where Z_{in} represents the input impedance, Z_0 is the impedance of free space, and Z is the normalized input impedance related to the impedance in free space; μ_r and ε_r are the relative complex permeability and permittivity of the absorber; f, d and c are frequency of electromagnetic wave, coating thickness and light velocity in free space, respectively.

3 RESULTS AND DISCUSSION

3.1 Characteristics of microwires

3.1.1 Structural characterization

The SEM images (*cf.* Fig. 1a, 1b) of a glass-coated microwire indicates that the wire has regular surface, uniform diameter and, after glass removal by HF acid, the metallic core is still smooth and without obvious corrosion cavity, which should have little influence on decreasing the mechanical property of the wire. The total diameter of the glass-coated microwire is 29 μm whilst the glass coating thickness is 4 μm.

The XRD features along with magnetic properties were summarized in Figure 2. Figure 2a shows the XRD patterns of as-cast microwires and treated micorwires by glass removal and joule annealing at 66 mA and 132 mA for 15 min, respectively. It is seen that for all the samples, only one broad diffuse peak is observed at the angle of 45°, which presents a typical amorphous broad halo pattern, except that AMW-132 which indicates that a partial cubic crystalline Fe_3Si phase (JCPDS file number 45-1207) has been formed and the grain size is about 30 nm evaluated by the JADE program (version 5.0, Materials Data Inc., Livermore, CA).

3.1.2 Magnetic properties

Figure 2b shows the longitudinal hysteresis loops of all samples. Obviously, after low current joule annealing, the soft magnetic properties of AMW-66 are far enhanced compared to MW, the coercivity (H_c) of which is about 1208 A/m. After 15 min annealing at 66 mA, the coercivity reaches the

minimum value of near 47 A/m, but increases to 3900 A/m at 132 mA resulted from the presence of large crystalline grains. To compare with joule annealing, microwires after glass removal were prepared. This also softens dramatically the magnetic properties of the microwires by diminishing the coercivity, indicating that part of the internal stress caused by the glass coating, which is concentrated at the outer shell, has played a dominating role in this result. It should be also observed that, compared to the AMW-66, GRMW has lower magnetic susceptibility due to the inhomogeneous distribution of internal stresses in the metallic core while joule annealing overcomes this issue by offering energy for internal stress redistribution and better defined microstructure and domain structure. Thus, the wires can be softer.

From the above analyses, it is clear that proper modifications of the internal stresses in the microwires by either glass removal or low current annealing can yield improvement of static magnetic properties. This is particularly crucial to realizing multifunctional microwire composites to meet both functional and structural requirements.

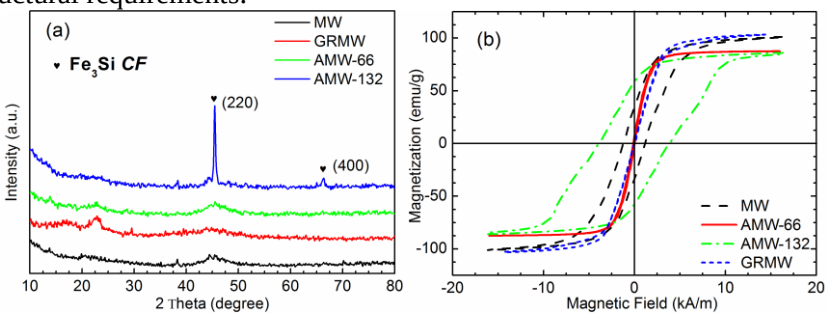

Fig. 2(Color online) (a) XRD patterns and (b) hysteresis loops of as-cast, glass-removed and annealed microwires

3.2 Electromagnetic constitutive parameters of rubber-based microwire composites

3.2.1 Influence of wire treatment on permittivity and permeability

By capitalizing on the outstanding characteristics of microwires as discussed above, multifunctional composites can be developed for different applications, especially for the purpose of microwave absorption in the present work. Thus, we prepared different composites embedded with 0.017 wt.% microwires (Fig. 1c) after different treatments and the distribution of microwires can be regarded as the grids with micorwires since the number of wires is countable.

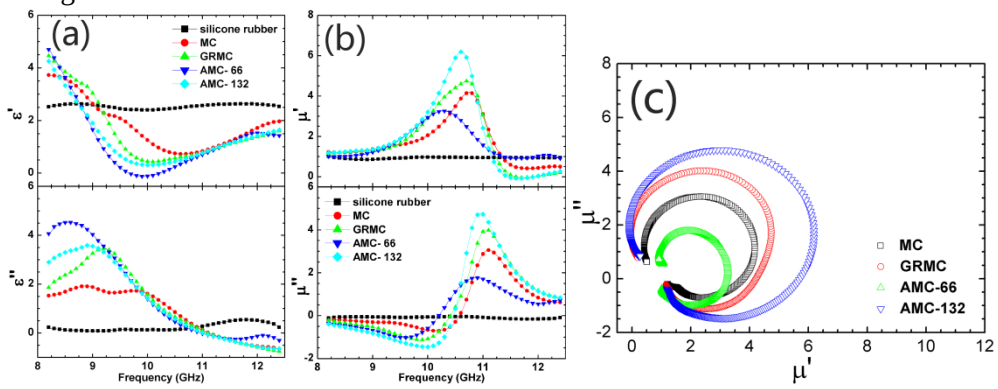

Fig. 3(Color online) (a) and (b) Complex permittivity and permeability spectra of composites and (c) Cole-Cole plot of μ" versus μ'

Referring to Fig. 3a-b, the samples embedded with microwires after glass removal and joule annealing show similar trends in both complex permittivity and permeability as the samples embedded with as-cast microwires. And the curves of permittivity and permeability show dielectric resonance and natural ferromagnetic resonance (NFMR), respectively. NFMR is mainly determined by the interaction of the circumferential field H_{circ} generated by the electric polarization and the axial

anisotropy field H_{ax} which depends on the sample length and can be several orders larger than the microwave field of the empty waveguide[4]. Additionally NFMR maintains the precession against the natural spin damping to an oscillating transverse field [17], here referred to as H_{circ}.

However, all the peaks of profiles of complex permeability or complex permittivity shift to lower frequency, in descending order of sample MC, GRMC, AMC-132 and AMC-66. The ε'' value of composites decreases in the order of AMC-66, AMC-132, GRMC and MC; however, both μ' and μ'' decrease from AMC-132, GRMC, MC to AMC-66. Since silicone rubber is non-magnetic and can be regarded as transparent to the X-band microwave, the embedded micorwires are directly responsible for both dielectric and magnetic properties of these composites.

For the complex permittivity, the dielectric resonance frequency $f_{res,n}$ of composites with low microwire concentration is given by[18]:

$$f_{res,n} = c(2n\text{-}1)/(2l\sqrt{\varepsilon}), \qquad (3)$$

where c is light velocity, n natural number, l microwire length, and ε is permittivity of the matrix taken as 2. Thus, in the present cases, $f_{res,n}$ is only related to the wire length, which should be the same. The inconsistency can be explained by the varying effective wire length.

As for the complex permeability, Fig. 3b shows the NFMR peaks in all samples. To further reveal the major loss mechanism due to NFMR, we draw the Cole-Cole plots of relative permeability (Fig. 3c), which appear as full circles for all samples[19], confirming that only the switching state[20] formed by magnetization reversal is dominant, during which process NFMR occurs. Details of associated reversal process are discussed in next section on microwave energy dissipation. The shift of NFMR peaks can be explained by Kittle's law [21]:

$$f_{FMR} = g\sqrt{(H_a + 4\pi M)(H_a + H)}/2\pi, \qquad (4)$$

where H_a is the magnetoelastic anisotropy field that can be estimated by the hysteresis loops, M is magnetization, g is gyromagnetic ratio and H is external applied magnetic field. Since there is no external magnetic field, f_{FMR} should shift to higher frequency as H_a increases.

Based on the hysteresis loops of different microwires in Fig. 2b, microwires obtain higher anisotropy in ascending order of AMW-66, GRMW, MW and AMW-132. However, AMC-132 has the second lowest f_{FMR} (shown in Fig. 3b) albeit the largest anisotropy field. Such inconsistency can be explained by the fact that annealing generates significant redistribution of the internal stress in wires in addition to the stress relief. This is in contrast to the non-uniform distribution of internal stress for as-cast and glass removed samples.

3.2.2 Influence of wire treatments on domain structure

The dispersion of electromagnetic constitutive parameters is closely linked to the magnetic features of the microwires. Hence, the magnetic behaviors of the wires depend strongly on the domain structure, which is determined by minimization of the magneto- elastic energy K_{me} for long wires and is given by:

$$K_{me} = \frac{3}{2}\lambda_s \sigma_{ii} \qquad (5)$$

where λ_s refers to saturation magnetostriction coefficient , σ_{ii} refers to the dominant internal stress component [22]. By different treatment, the internal stress of the wires can be either relieved or redistributed thus σ_{ii} changes; and by adjusting the microstructures of the wires, the magnetostriction changes, and thus the domain structures (Fig. 4) of the treated wires differ from each other. According to the hysteresis loops in Fig. 2e, λ_s of all the four wires remains negative.

For as-cast wires, with negative λ_s, and the calculated radial distribution of internal stresses of glass coated microwires in Ref.[22], the minimization of magnetoelastic energy controls the domain

structure with a radially magnetized inner core *IC* results from the coupling of large tensile stress σ_z (positive) and negative λ_s, and a circumferentially magnetized outer shell *OS* arises from the coupling of circumferential compressive stress σ_θ (negative) and negative λ_s. The radial magnetization from *IC* would lead to severe magnetostatic and exchange interactions so that the magnetization in this region is also axial but with small component.

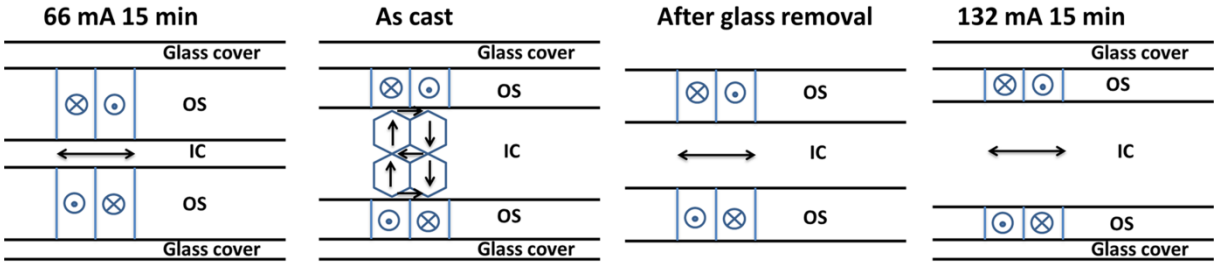

Fig. 4(Color online) domain structures of different wires

After treatment by glass removal or current annealing, as the absolute value of σ_z (positive) decreases but is still dominant in the IC region, the anisotropy of IC turns to be axial with less coupling of negative λ_s as well as the absolute value of σ_θ (negative) decreases thus the circumferential anisotropy of OS is better modified locally. After glass removal, σ_θ is not as much relieved as σ_z because the axial internal stress induced by glass coating is the largest component, so the σ_z (zero) moves to the inner region, thus the volume of IC decreases more than MW, while that of the *OS* remains circumferential. For AMW-66, σ_θ is still not as much relieved as σ_z whilst the circumferential anisotropy of OS is better modified by the circumferential magnetic field generated by the DC current, hence the volume fraction of the *IC* decreases further compared to GRMW. For AMW-132, similar to AMW-66, the OS remains circumferential. However with higher current, σ_θ is more relieved than σ_z, so the σ_θ (zero) moves to the surface region, thus the volume of IC increases more than MW. It should be noted that the ratio of the inner core radius to the whole metallic core radius can be approximated as the ratio of remnant magnetization to saturation magnetization [23]. According to remanence of the wires shown in Fig. 2b, the volume of IC discussed above is consistent with the ratio of remnant magnetization of the wires.

Consequently, the surface impedance is increased in ascending order of AMW-66, AMW-132, GRMW and MW owing to both larger volume of OS and better modified circumferential anisotropy. As the distribution of the wires can be regarded as grids, the composites can also be simplified to an equivalent material slab, the effective permittivity, ε_{eff}, of which can be calculated by a theoretical model of Liberal et al. [24], is proportional to surface impedance[25]. Indeed, Fig.3a reveals that the intensity of ε" is consistent with the surface impedance.

On the magnetic permeability front, the *IC* axial anisotropy of the wire increases in the order of AMW-66, MW, GRMW and AMW-132, which is consistent with the magnitudes of the NFMR peaks of composites filled with corresponding wires.

It can be concluded that the complex permittivity and permeability of microwire composites are related to the wire domain structure, which is mainly governed by the internal stress and their distribution since λ_s stays negative.

3.3 Microwave absorbing properties of composites with treated microwires

Basically, microwave absorbing property depends on dielectric loss or magnetic loss or both [1]. The calculated reflection loss of composites with thickness of 1 mm (Fig. 5a) shows that all composite samples have a similar trend, and AMC-132 has the least reflection loss of -22.8 dB at 11.2 GHz and broadest absorption bandwidth (0.62 GHz) with reference to -10 dB, which means 90% incident microwave can be absorbed. The minimum reflection losses and absorption bandwidth with reference

to -10 dB of GRMC, MC and AMC-66 are -18.4 dB (0.575 GHz), -12.3 dB (0.35 GHz) and -6.5 dB, in agreement with the magnitudes of the complex permeability in Fig. 3b. The absorption frequency (f_{peak}^{RL}) shifts towards lower frequency, consistent with f_{FMR} shown in Fig. 3b, confirming the absorption performance arises mainly from the magnetic loss.

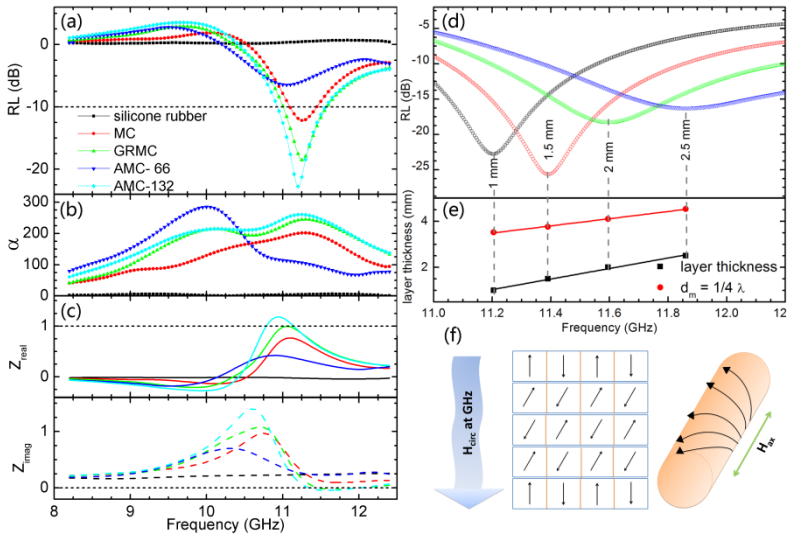

Fig. 5(Color online) (a) Calculated reflection loss; (b) attenuation constant; (c) Zreal and Zimag for 1 mm thick composites; (d) variations of RL curves versus frequency for AMC-132; (e) simulation of dm versus fm for AMC-132 with different thickness; and (f) microscopic schematic diagram of microwave absorption.

In the present study, the AC permeability is dictated by the evolution of the domain structure in the context of aforementioned natural ferromagnetic resonance frequency. A schematic diagram is interpreted in Fig. 5f. NFMR is induced during the magnetization reversal process consisting of domain rotation and reversal. Upon application of a high frequency electric field, the circumferential H_{circ} triggers the rotation of magnetization in the surface circular domains to an inclined meta-stable state whose angle is controlled by frequency[26]. The larger the axial anisotropy, the more energy is needed to overcome the axial anisotropy. As the frequency becomes higher, an increase of the amplitude of vibration of the magnetization is induced. When this overcomes the axial anisotropy of the wire, the rotated domain changes its sign; which is considered as domain reversal governed by damping that varies with composition[22]. During magnetization reversal energy is consumed. As mentioned before, AMW-132 has the largest axial anisotropy, and AMW-66 the smallest, which is consistent with the minimum RL values of corresponding composites.

Since microscopic microwave absorption is caused by the NFMR induced during magnetization reversal, we need to further explore the exact macroscopic mechanisms to fully understand microwave absorption. Three major macroscopic mechanisms are considered: intrinsic microwave attenuation property of materials, impedance matching mechanism and quarter-wavelength matching mechanism.

For the first mechanism, according to the transmission line theory and microwave propagation constant, the microwave attenuation performance of materials is determined by the attenuation constant (α) [27]:

$$\alpha = (\sqrt{2}\pi f/c) \times \sqrt{\left(\mu''\varepsilon'' - \mu'\varepsilon'\right) + \sqrt{(\mu''\varepsilon'' - \mu'\varepsilon')^2 + (\varepsilon'\mu'' + \varepsilon''\mu')^2}} \quad (7)$$

It is clear that α is independent of sample thickness but varies with frequency since permeability and permittivity frequency-dependent. Fig. 5b shows that AMC-132 has the largest attenuation constant in the high frequency range, exhibiting the best microwave absorption performance. The

order of the attenuation constant α (f_{peak}^{RL}) is consistent with the magnitudes of reflection loss in Fig. 5a. Also, the peak frequency of the attenuation constant (f_{peak}^{α}) is near f_{peak}^{RL} except for AMC-66, indicating the microwave absorbing capacity is related to the attenuation constant.

Apart from the intrinsic microwave attenuation property which mainly comes from the magnetic loss, the microwave parameter matching condition has been proven to be important for better microwave absorption performance, which can be defined when the normalized input impendence Z is unity. The peak frequencies, RL values, attenuation constant and calculated impedance at f_{peak}^{RL} of samples and their corresponding f_{peak}^{α} are listed in Table 3. When the thickness of the composites is 1 mm, for AMC-132, the real part of impedance (Z_{real}) calculated at f_{peak}^{RL} is 0.915, whist the imaginary part of impedance (Z_{imag}) is 0.11, which is the most matching of four samples (Fig. 5c). Clearly, the matching condition gets worse in the order of AMC-132, GRMC, MC and AMC-66 at their corresponding frequency (f_{peak}^{RL}). So, it is understandable that although AMC-66 exhibits the highest attenuation constant α (285 at 10.01 GHz), there is no absorption peak owing to the poor matching condition where Z_{real} is -0.08, and Z_{imag} is 0.63 (shown in Fig. 5c). The relative importance of impedance matching over attenuation constant is further revealed in Table 4, which shows the calculated attenuation constant and impedance at f_{peak}^{RL} of AMC-132 with different thickness d. Combining Table 4 with Fig. 5d, it is obvious that when the thickness is 1.5 mm, RL reaches the minimum value, which is -25.7 dB at 11.39 GHz, where Z_{real} is 1.026 and Z_{imag} is -0.102, yielding the best matching condition. Although 1 mm thick sample has the largest attenuation constant at 11.205 GHz which reaches a minimum RL -22.8 dB, its matching condition is not as good as 1.5 mm thick sample and hence offers weaker microwave absorption.

Sample	f_{peak}^{RL}(GHz)	RL (dB)	α	Z_{real}	Z_{imag}
MC	11.26	-12.2	201.5	0.692	0.289
GRMC	11.255	-18.5	244.6	0.848	0.159
AMC-66	10.995	-6.5	114.6	0.411	0.364
AMC-132	11.205	-22.8	260.5	0.915	0.110

Table 3 Peak frequency, RL value, attenuation constant and calculated impedance at f_{peak}^{RL} of samples in 1 mm thickness

d (mm)	f_{peak}^{RL}(GHz)	RL (dB)	d_m (mm) (d_m =λ/4)	α	Z_{real}	Z_{imag}
1	11.205	-22.8	3.5	260.5	0.915	0.110
1.5	11.39	-25.7	3.8	255.4	1.026	-0.102
2	11.595	-18.3	4.1	235.9	0.972	-0.24
2.5	11.86	-16.3	4.5	201.6	0.850	-0.244

Table 4 Peak frequency, RL value, calculated matching thickness, attenuation constant and impedance at f_{peak}^{RL} of AMC-132

Additionally, the quarter-wavelength matching mechanism has also been widely employed to discuss the frequency dependence of ferrite composites with thickness. The matching thickness (d_m) and the corresponding peak frequency (f_m) should satisfy the following equation [28]:

$$d_m = n\lambda/4 = nc/(4f_m\sqrt{|\mu_r||\varepsilon_r|}) \quad (n = 1, 3, 5, \ldots), \qquad (8)$$

where $|\varepsilon_r|$ and $|\mu_r|$ are modulus of the measured complex permittivity and permeability at f_m, respectively. In view of the $\lambda/4$ model, when the matching thickness of absorber satisfies the above formula, at some special frequency, two reflected waves from the air - absorber and absorber - metal interfaces are out of phase by 180° and cancel each other.

Figure 5d and 5e shows variations of RL curves versus frequency with different thicknesses d and

simulations of d_m versus f_m for AMC-132, respectively. Obviously, the real layer thickness d of the sample is far away from matching the calculated thickness d_m. Another remarkable feature is that, at lower frequency than peak frequency, the magnitudes of ε', ε", μ' and μ" are all proportional to frequency (shown in Fig. 3a and 3b), resulting in a thin matching thickness d_m at relatively low frequency (shown in Fig. 5e). This differs from conventional cases and will be very useful for development of low-frequency absorbers which remains a great challenge. It must be emphasized that to obtain thinner magnetic absorbers for lower frequency applications, it is necessary to improve the imaginary part of permittivity and/or decrease the imaginary part of permeability slightly in order not to compromise the absorbing ability to reach close impedance matching. To achieve this goal, high dielectric loss materials such as carbon nanotubes or graphenes can be added to the present system. Alternatively, one of the unique merits of microwires as discussed above is that the magnitude of internal stress and stress distribution can be manipulated somewhat freely without necessarily conforming to Snoek's law. This paves a way to a multiscale design of a microwave absorber from microscale (local filler) to mesoscale (arrangement of fillers) to macroscale (composite architecture).

In summary, it can be concluded that the microwave absorbing property of the wire composites comes mainly from the magnetic loss that is determined by both the intrinsic microwave attenuation property and impedance matching condition, especially the latter is more dominating than the former. When the matching condition is poor, microwave absorption is not good in spite of a large attenuation constant. By contrast, under perfect matching condition, microwave absorption can be greatly increased even the attenuation constant is ordinary.

4 CONCLUSIONS

In this work, we found that microwires are effective X-band absorbents dominated by magnetic loss. A careful selection of aspect ratio and suitable treatments of the microwires are important in optimizing the microwave absorption performance. Particularly internal stress modulation has shown profound effects in controlling the microwave absorption frequency and intensity of these wire composites by tailoring the domain structure and local anisotropy field which can be varied by joule heating and glass removal strategies. Composites with very low loading (0.017 wt.%) of microwires annealed at 132 mA for 15 min and large aspect ratio (9 mm length) have much better microwave absorption due to their better intrinsic microwave attenuation property and impedance matching condition. Microwave absorbing mechanism in the wire composites has been discussed (a) microscopically by detailing the process of domain rotation and reversal caused by the electromagnetic field; and (b) macroscopically by examining the relative effect of the intrinsic microwave attenuation property of materials and impedance matching. Most importantly, in (a), at the micro level, the magnitude of internal stress and stress redistribution can be manipulated readily; in (b), impedance matching is more important than attenuation. Finally, failure of the quarter-wavelength model to describe the absorption frequency versus matching thickness relationship offers possibility to tackle the low frequency absorption challenge imposed by thickness constraint.

ACKNOWLEDGEMENTS

FXQ would like to thank the financial support of NSFC No. 51501162 and No. 51671171, ARC DE160101167 and the National Youth Thousand Talent Program of China. PHX would like to thank ZNSFC No. 2016C34005. Microwave measurement support provided by Mr. Jiabin Xi and Professor Chao Gao is acknowledged by all authors.

REFERENCES

[1] F. Qin and C. Brosseau, "A review and analysis of microwave absorption in polymer composites filled with carbonaceous particles," *Journal of Applied Physics*, vol. 111, no. 6, p. 061301, 2012.

[2] M.-H. Phan and H.-X. Peng, "Giant magnetoimpedance materials: Fundamentals and applications," *Progress in Materials Science*, vol. 53, no. 2, pp. 323-420, February 2008.

[3] F. X. Qin and H. X. Peng, "Ferromagnetic microwires enabled multifunctional composite materials.," *Progress in Materials Science*, vol. 58, no. 2, pp. 183-259, 2013.

[4] P. Marin, D. Cortina, and A. Hernando, "Electromagnetic Wave Absorbing Material Based on Magnetic Microwires," *IEEE Transactions on Magnetics*, vol. 44, no. 11, pp. 3934-3937, 2008.

[5] P. Marín, D. Cortina, and A. Hernando, "High-frequency behavior of amorphous microwires and its applications," *Journal of Magnetism and Magnetic Materials*, vol. 290-291, no. Part 2, pp. 1597-1600, 2005.

[6] H. Chiriac, T. A. Ovari, and G. Pop, "Internal stress distribution in glass-covered amorphous magnetic wires," *Physical Review B*, vol. 52, no. 14, p. 10104, 1995.

[7] H. Chiriac and T. A. Óvári, "Magnetic properties of amorphous glass-covered wires," *Journal of Magnetism and Magnetic Materials*, vol. 249, no. 1–2, pp. 46-54, 2002.

[8] V. Zhukova *et al.*, "Tailoring of magnetic properties of glass-coated microwires by current annealing," *Journal of Non-Crystalline Solids*, vol. 287, no. 1-3, pp. 31-36--, 2001.

[9] F. X. Qin *et al.*, "Exceptional EMI shielding properties of ferromagnetic microwires enabled polymer composites," *Journal of Applied Physics*, vol. 108, p. 044510, 2010.

[10] F. X. Qin, H. X. Peng, J. Fuller, and C. Brosseau, "Magnetic field-dependent effective microwave properties of microwire-epoxy composites," *Applied Physics Letters*, vol. 101, no. 15, p. 152905, 2012.

[11] Z. Zhang, C. Wang, Y. Zhang, and J. Xie, "Microwave absorbing properties of composites filled with glass-coated Fe69Co10Si8B13 amorphous microwire," *Materials Science and Engineering B*, vol. 175, no. 3, pp. 233-237, 2010.

[12] V. S. Larin, A. V. Torcunov, A. Zhukov, J. Gonzalez, M. Vazquez, and L. Panina, "Preparation and properties of glass-coated microwires," *Journal Of Magnetism And Magnetic Materials*, vol. 249, no. 1-2, pp. 39-45, 2002.

[13] R. B. Marks, J. A. Jargon, and J. R. Juroshek, "Calibration Comparison Method for Vector Network Analyzers," in *48th ARFTG Conference Digest*, 1996, vol. 30, pp. 38-45.

[14] A. M. Nicolson and G. F. Ross, "Measurement of the Intrinsic Properties of Materials by Time-Domain Techniques," *IEEE Transactions on Instrumentation and Measurement*, vol. 19, no. 4, pp. 377-382, 1970.

[15] D. P. Makhnovskiy, L. V. Panina, C. Garcia, A. P. Zhukov, and J. Gonzalez, "Experimental demonstration of tunable scattering spectra at microwave frequencies in composite media containing CoFeCrSiB glass-coated amorphous ferromagnetic wires and comparison with theory," *Physical Review B: Condensed Matter*, vol. 74, no. 6, p. 064205, 2006.

[16] Y. Naito and K. Suetake, "APPLICATION OF FERRITE TO ELECTROMAGNETIC WAVE ABSORBER AND ITS CHARACTERISTICS," *Ieee Transactions on Microwave Theory and Techniques*, vol. MT19, no. 1, pp. 65-&, 1971.

[17] P. Ciureanu *et al.*, "Study of the complex permeability of amorphous wires using microwave impedance spectroscopy," in *Microwave Conference, 1999 Asia Pacific*, 1999, vol. 3, pp. 876-879 vol.3.

[18] D. P. Makhnovskiy and L. V. Panina, "Field dependent permittivity of composite materials containing ferromagnetic wires," *Journal of Applied Physics*, vol. 93, no. 7, pp. 4120-4129, 2003.

[19] R. Valenzuela, H. Montiel, M. P. Gutiérrez, and I. Betancourt, "Characterization of soft ferromagnetic materials by inductance spectroscopy and magnetoimpedance," *Journal of Magnetism and Magnetic Materials*, vol. 294, no. 2, pp. 239-244, 2005.

[20] W. Kleemann, J. Rhensius, O. Petracic, J. Ferre, J. P. Jamet, and H. Bernas, "Modes of periodic domain wall motion in ultrathin ferromagnetic layers," *Phys Rev Lett*, vol. 99, no. 9, p. 097203, Aug 31 2007.

[21] P. Marín, D. Cortina, and A. Hernando, "High-frequency behavior of amorphous microwires and its applications," *Journal of Magnetism and Magnetic Materials*, vol. 290-291, pp. 1597-1600, 2005.

[22] H. Chiriac, T. A. Óvári, and A. Zhukov, "Magnetoelastic anisotropy of amorphous microwires," *Journal of Magnetism and Magnetic Materials*, vol. 254–255, pp. 469-471, 2003.

[23] M. Vázquez and A. P. Zhukov, "Magnetic properties of glass-coated amorphous and nanocrystalline microwires," *Journal Of Magnetism And Magnetic Materials*, vol. 160, pp. 223-228, 1996.

[24] I. Liberal, I. Nefedov, I. Ederra, R. Gonzalo, and S. Tretyakov, "Electromagnetic response and homogenization of grids of ferromagnetic microwires," *Journal of Applied Physics*, vol. 110, p. 064909, 2011.

[25] A. Yelon, D. Menard, M. Britel, and P. Ciureanu, "Calculations of giant magnetoimpedance and of ferromagnetic resonance response are rigorously equivalent," *Applied Physics Letters*, vol. 69, no. 20, pp. 3084-3085, 1996.

[26] A. Chizhik *et al.*, "Transformation of magnetic structure in amorphous microwires induced by temperature and high frequency magnetic field," *Journal of Alloys and Compounds*, vol. 632, pp. 520-527, 2015.

[27] J. Feng, F. Pu, Z. Li, X. Li, X. Hu, and J. Bai, "Interfacial interactions and synergistic effect of CoNi nanocrystals and nitrogen-doped graphene in a composite microwave absorber," *Carbon*, vol. 104, pp. 214-225, 2016.

[28] B. Wang, J. Wei, Y. Yang, T. Wang, and F. Li, "Investigation on peak frequency of the microwave absorption for carbonyl iron/epoxy resin composite," *Journal of Magnetism and Magnetic Materials*, vol. 323, no. 8, pp. 1101-1103, 2011.